Physics Letters B 834 (2022) 137382

Contents lists available at ScienceDirect

Physics Letters B

www.elsevier.com/locate/physletb

Flavor hierarchies, flavor anomalies, and Higgs mass from a warped extra dimension

Javier Fuentes-Martín [a], Gino Isidori [b,*], Javier M. Lizana [b], Nudžeim Selimović [b], Ben A. Stefanek [b]

[a] Departamento de Física Teórica y del Cosmos, Universidad de Granada, E–18071 Granada, Spain
[b] Physik-Institut, Universität Zürich, CH-8057 Zürich, Switzerland

ARTICLE INFO

Article history:
Received 14 April 2022
Received in revised form 29 June 2022
Accepted 16 August 2022
Available online 27 August 2022
Editor: G.F. Giudice

ABSTRACT

The recent B-meson anomalies are coherently explained at the TeV scale by *4321 gauge models* with hierarchical couplings reminiscent of the Standard Model Yukawas. We show that such models arise as the low-energy limit of a complete theory of flavor, based on a warped fifth dimension where each Standard Model family is quasi-localized on a different brane. The Higgs is identified as a pseudo-Nambu-Goldstone boson emerging from the same dynamics responsible for 4321 symmetry breaking. This novel construction unifies quarks and leptons in a flavor non-universal manner, provides a natural description of flavor hierarchies, and addresses the electroweak hierarchy problem.

1. Introduction

The deviations from lepton flavor universality observed in neutral-current [1–4] and charged-current [5–10] semileptonic B decays have stimulated intense model-building activity, triggering new ideas about the ultraviolet (UV) completion of the Standard Model (SM). Two key aspects have emerged quite clearly from the early attempts to provide a combined explanation of the two sets of anomalies: i) a possible common origin of flavor anomalies and Yukawa hierarchies [11], as hinted by the approximate $U(2)^n$ flavor structure of new physics [12,13], ii) the necessity of new degrees of freedom at the TeV scale coupled mainly to the SM third generation, hinting at a possible link with the electroweak (EW) hierarchy problem [14,15].

In this letter, we show how these two aspects can be consistently combined within a five-dimensional (5D) model. The three main assumptions of our construction, and their motivations, can be listed as follows:

I. *4321 gauge symmetry above the TeV scale.* The most effective mediator to address both sets of anomalies is a TeV-scale U_1 leptoquark [13,16–19]. This field can be identified with one of the broken generators of the fundamental gauge group $SU(4)_h \times SU(3)_l \times SU(2)_L \times U(1)_X$, denoted 4321 group [20]. Here $SU(2)_L$ acts as in the SM and hypercharge is a combination of $U(1)_X$ and the T_{15} generator of $SU(4)_h$. Color is the diagonal subgroup of $SU(4)_h \times SU(3)_l$, and the labels h and l indicate the flavor non-universal assignment of the SM fermions under this part of the gauge group, resulting in a U_1 coupled mainly to third-generation fermions [11,21]. Apart from the U_1, two EW-neutral gauge bosons acquire mass from the 4321 breaking: a color-octet, G', and a singlet, Z'. The presence of these two mediators does not alter the U_1 solution of the anomalies [22–24].

II. *Flavor hierarchies from a 3-brane structure in 5D.* The hierarchies in both the Yukawa and U_1 couplings, i.e. the breaking of the approximate $U(2)^n$ flavor symmetry acting on the light families at the TeV scale, emerge from a multi-scale construction [11,25–27] that, in turn, can be viewed as the effect of a 3-brane structure in 5D. The strong constraints on flavor-violating terms involving the light families naturally point toward a warped geometry [28]. The size of the Yukawa couplings implies $kL \approx 10$ [28], where L is the distance between the infrared (IR) (3^{rd} gen.) brane and the most UV (1^{st} gen.) brane, and k is the 5D curvature constant.

III. *Holographic Higgs.* The SM Higgs can be realized as a pseudo-Nambu-Goldstone boson (pNGB) emerging from the same dynamics responsible for the breaking of $SU(4)_h \times SU(3)_l$ [15]. In the warped 5D description, this can be achieved via gauge-Higgs unification [29], realized by extending the EW part of the bulk gauge symmetry. For the sake of simplicity and minimality, we assume

* Corresponding author.
E-mail addresses: javier.fuentes@ugr.es (J. Fuentes-Martín), isidori@physik.uzh.ch (G. Isidori), jlizana@physik.uzh.ch (J.M. Lizana), nudzeim@physik.uzh.ch (N. Selimović), bestef@physik.uzh.ch (B.A. Stefanek).

https://doi.org/10.1016/j.physletb.2022.137382

Table 1
Matter content. Here, $i = 1, 2, 3$ and $j = 1, 2$. The upper block refers to fermion fields, the lower block to scalars.

Field	$SU(4)_h$	$SU(4)_l$	$SO(5)$	$U(1)_\Psi$	$U(1)_\mathcal{S}$
$\Psi^3, \Psi^3_d, \mathcal{X}^{(\prime)}$	**4**	**1**	**4**	1	0
$\Psi^j, \Psi^j_{u,d}$	**1**	**4**	**4**	1	0
$\mathcal{S}^i$	**1**	**1**	**1**	0	1
Σ	**1**	**1**	**5**	0	0
Ω	**1**	**4**	**4**	1	-1
Φ	**1**	**1**	**1**	0	2

$$\begin{aligned} \mathcal{G}^{23}_{\rm bulk} &\equiv SU(4)_h \times SU(3)_l \times U(1)_l \times SO(5)\,, \\ \mathcal{G}_{\rm IR} &\equiv SU(3)_c \times U(1)_{B-L} \times SO(4)\,, \end{aligned} \tag{1}$$

where $SU(3)_c$ and $U(1)_{B-L}$ are flavor-universal subgroups of $SU(4)_h \times SU(3)_l \times U(1)_l$, and the 23 bulk is the most IR side of the bulk (see Fig. 1). The fifth component of the gauge fields associated to the $SO(5)/SO(4)$ coset contains four pNGB zero modes transforming as a **4** of $SO(4)$ that we identify with the SM Higgs field, thus realizing the minimal composite Higgs scenario [30].

2. The 5D model

We consider a 5D model with a warped compact extra dimension containing three branes (similar to the one explored in [31]) with two positive and one negative tension branes (++−). The metric is

$$ds^2 = e^{-2\sigma(y)}\,\eta_{\mu\nu}\,dx^\mu dx^\nu - dy^2\,, \tag{2}$$

where, in the absence of backreaction from scalar fields, the warp factor $\sigma(y)$ is

$$\sigma(y) = \begin{cases} \sigma_1(y) = k_1 y & 0 \le y \le \ell \\ \sigma_2(y) = k_1\ell + k_2(y-\ell) & \ell \le y \le L \end{cases}. \tag{3}$$

Here L denotes the total length of the compact extra dimension and ℓ the location of the intermediate brane. Due to the tension of the branes, $k_1 \le k_2$. For simplicity, in what follows we assume $k_1 = k_2 \equiv k$, corresponding to a zero middle brane tension. This multi-brane setup can be stabilized via a straight-forward extension of the Goldberger-Wise (GW) mechanism [32,33], with suitable brane-localized potentials for the GW scalar [34].

Beside the IR bulk and brane symmetries specified in (1), we assume

$$\begin{aligned} \mathcal{G}^{12}_{\rm bulk} &\equiv SU(4)_h \times SU(4)_l \times SO(5)\,, \\ \mathcal{G}_{\rm UV} &\equiv SU(4)_h \times SU(3)_l \times U(1)_l \times SU(2)_L \times U(1)_R\,, \end{aligned} \tag{4}$$

where $\mathcal{G}_{\rm UV}$ and $\mathcal{G}^{12}_{\rm bulk}$ are the gauge symmetries in the most UV brane and the UV side of the bulk, respectively. The middle brane is therefore a discontinuity corresponding to the symmetry-breaking pattern $SU(4)_l \to SU(3)_l \times U(1)_l$. Alternatively, we could have chosen $\mathcal{G}^{12}_{\rm bulk} = \mathcal{G}^{23}_{\rm bulk}$, with no difference in the low-energy phenomenology. In this case, light-family quark-lepton unification could take place in a bulk between a deeper UV brane (e.g. the Planck brane) and the first-family brane.

The chosen gauge symmetries yield $15 + 4$ pNGBs, 15 of which become the longitudinal components of the 4321 gauge bosons, U_1, G' and Z', which acquire a degenerate mass of $M_{15} \approx \Lambda_{\rm IR}\sqrt{2/(kL)}$ [35], with $\Lambda_{\rm IR} \approx k e^{-kL}$. This mass generation mechanism (similar to the one in [15]), yields a mass gap between the 4321 gauge bosons and the lightest vector resonances of the Kaluza-Klein (KK) tower, namely $M_{\rm KK}/M_{15} \approx \sqrt{2kL}$. The remaining pNGBs correspond to the SM Higgs field: $H \sim (\mathbf{1}, \mathbf{2})_{1/2}$.

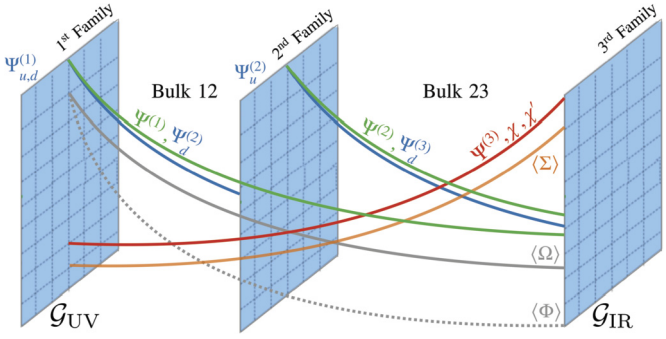

Fig. 1. Schematic structure of the extra dimension including fermion zero-mode and scalar VEV profiles.

The matter fields and their corresponding transformation properties under the 12-bulk gauge symmetry are listed in Table 1. We embed all fermion fields (except $\mathcal{S}^i$) into the spinorial **4** representation of $SO(5)$, which contains two (complex) doublets, one transforming in the fundamental of $SU(2)_L$ and the other in the fundamental of $SU(2)_R$. These fermions are also embedded into fundamental representations of $SU(4)_{h,l}$ forming quark-lepton multiplets à la Pati-Salam. The boundary conditions (BCs) for the fermions are chosen as follows

$$\begin{aligned} \Psi^3 &= \begin{bmatrix} \psi^3\,(+,+) \\ \psi^3_u\,(-,-) \\ \tilde\psi^3_d\,(+,-) \end{bmatrix}, \qquad \Psi^3_d = \begin{bmatrix} \tilde\psi^3\,(+,-) \\ \tilde\psi^3_u\,(+,-) \\ \psi^3_d\,(-,-) \end{bmatrix}, \\ \mathcal{X}^{(\prime)} &= \begin{bmatrix} \chi^{(\prime)}(\pm,\pm) \\ \chi^{(\prime)}_u(\mp,\pm) \\ \chi^{(\prime)}_d(\mp,\pm) \end{bmatrix}, \qquad \Psi^j = \begin{bmatrix} \psi^j\,(+,+) \\ \tilde\psi^j_u\,(-,+) \\ \tilde\psi^j_d\,(-,+) \end{bmatrix}, \\ \Psi^j_u &= \begin{bmatrix} \tilde\psi^j\,(+,-) \\ \psi^j_u\,(-,-) \\ \hat\psi^j_d\,(+,-) \end{bmatrix}, \qquad \Psi^j_d = \begin{bmatrix} \hat\psi^j\,(+,-) \\ \hat\psi^j_u\,(+,-) \\ \psi^j_d\,(-,-) \end{bmatrix}, \end{aligned} \tag{5}$$

and $\mathcal{S}^i = S^i(+,+)$, where we decomposed the spinorial $SO(5)$ multiplets into $SU(2)_L$, up-type $SU(2)_R$ and down-type $SU(2)_R$ components, as required by the $SU(2)_L \times U(1)_R$ symmetry in the UV. The resulting zero modes correspond to the SM field content (including three right-handed neutrinos), ψ^i_L and $\psi^i_{uR,dR}$ with quarks and leptons unified in $SU(4)$ representations, one vector-like representation χ_L and χ'_R, and three chiral SM singlets S^i_L. The SM-singlet fermions, the scalars Ω and Φ, and the (global) $U(1)_\mathcal{S}$ symmetry are needed to give neutrinos masses via an inverse see-saw mechanism [28]. The Ω field is also responsible for the spontaneous breaking of the UV gauge symmetry down to the 4321 symmetry, where the $U(1)$ factor in 4321 is the diagonal subgroup of $U(1)_l \times U(1)_R$. Furthermore, the Ω field can play the role of the GW scalar by appropriately choosing its brane-localized potentials and bulk masses. The scalar Σ plays a key role in generating the light Yukawa couplings, as discussed below. Finally, the (global) $U(1)_\Psi$ symmetry [36] is introduced to forbid baryon and lepton number violating higher-dimensional operators, already present in the Randall-Sundrum (RS) model [37] (see e.g. [38]).

2.1. Flavor hierarchies

As we discuss in what follows, *all* flavor hierarchies in the Yukawas and vector-like masses are explained with $\mathcal{O}(1)$ parameters by assuming the fermion localizations illustrated in Fig. 1, with $kL \approx 10$ and $k\ell \approx 4$. While there is some freedom in the choice

of fermion bulk masses that do not affect the solution to the flavor hierarchies, we take the following benchmark for concreteness (with $c_i \equiv M_i/k$ and M_i the corresponding fermion mass)

$$c^{(1,2)}_{\Psi^3} = c^{(1,2)}_{\mathcal{X}} = c^{(1)}_{\Psi^3_d} = c^{(1)}_{\Psi^2} = c^{(1)}_{\Psi^2_u} = 0\,,\ c^{(1,2)}_{\mathcal{X}'} = -1/2\,,$$
$$c^{(1,2)}_{\Psi^1} = c^{(2)}_{\Psi^2} = -c^{(2)}_{\Psi^3_d} = -c^{(1)}_{\Psi^2_d} = 1\,,\ c^{(1,2)}_{\Psi^1_{u,d}}, c^{(2)}_{\Psi^2_{u,d}} \leq -2\,. \tag{6}$$

Here and in the following the superscript (1) and (2) refer to the 12-bulk and 23-bulk, respectively. Even though the gauge symmetry in the 23-bulk is $SU(4)_h \times SU(3)_l$, for simplicity we choose $SU(4)$ symmetric bulk masses for this benchmark. Furthermore, we fix $\Lambda_{\rm IR} = 8$ TeV such that $M_{15} = 3.6$ TeV, which provides a good benchmark for the explanation of the B anomalies [22–24].

2.1.1. Vector-like masses and fermion mixing

The following mass terms are added on the IR brane

$$\mathcal{L}_{\rm IR} \supset \left(\bar{\mathcal{X}}_L \tilde{M}_\chi + \bar{\Psi}^3_L \tilde{M}_\Psi + \bar{\Psi}^j_L \tilde{m}^j_\psi\right) \mathcal{P}_L \mathcal{X}'_R\,, \tag{7}$$

in order to generate a vector-like mass among the zero modes. Here $\mathcal{P}_{L,R}$ is a projector into the $SU(2)_{L,R}$ components of the $SO(5)$ multiplets, and the IR masses decompose as $\tilde{M}_i = {\rm diag}(\tilde{M}^q_i, \tilde{M}^q_i, \tilde{M}^q_i, \tilde{M}^\ell_i)$ in $SU(4)$ space. These mass terms mix all the left-handed components of the zero modes, leaving the SM fermion content as massless chiral fields (plus the SM singlets needed for the inverse see-saw). The vector-like masses thus induced read

$$\mathcal{L} \supset -M_f\, \bar{f}_L \chi'_R\,,\ \ M_f = \Lambda_{\rm IR}\, \tilde{M}_f\, P\big(\{c^{(n)}_f\}, \{c^{(n)}_{\mathcal{X}'}\}\big)\,, \tag{8}$$

where $P(\{c_1\},\{c_2\})$ is a fermion profile function [39]. The behavior of the profile function is such that, for the fermion profiles in (6), we have

$$\Lambda_{\rm IR}\, P\big(\{c^{(n)}_{\Psi^j}\}, \{c^{(n)}_{\mathcal{X}'}\}\big) \sim \frac{\Lambda_{\rm IR}}{\sqrt{kL}}\, e^{k(\ell_j - L)/2} \approx 2\ {\rm TeV} \times V_{j3}\,,$$
$$\Lambda_{\rm IR}\, P\big(\{c^{(n)}_{\Psi^3,\mathcal{X}}\}, \{c^{(n)}_{\mathcal{X}'}\}\big) \sim \frac{\Lambda_{\rm IR}}{\sqrt{kL}} \approx 2\ {\rm TeV}\,, \tag{9}$$

where ℓ_j is the position of the j-th brane, and V_{ij} are Cabibbo–Kobayashi–Maskawa (CKM) matrix elements. We thus obtain TeV-scale vector-like masses with a $U(2)$-like mixing structure for the assumed benchmark, hence reproducing the required conditions for a successful explanation of the B-meson anomalies [22–24].

2.1.2. Yukawa couplings

Yukawa couplings with the Higgs are generated via three distinct mechanisms, depending on the fermions, giving rise to decreasing effective interactions:

I. *Top Yukawa.* The fermion BCs in (5) have been chosen such that, in the absence of IR masses, only the third-generation up-type Yukawa is generated:

$$\mathcal{L} \supset -y^{33}_u\, \bar{\psi}^3_L H \psi^3_{uR}\,,\ y^{33}_u = \frac{g_*}{2\sqrt{2}}\, P\big(\{c^{(n)}_{\Psi^3}\}, \{c^{(n)}_{\Psi^3}\}\big)\,, \tag{10}$$

where g_* is the $SO(5)$ KK coupling. In the absence of fermion mixing effects, y^{33}_u becomes the top Yukawa, y_t. Since $P(\{c^{(n)}_{\Psi^3}\}, \{c^{(n)}_{\Psi^3}\}) \lesssim 1$, we infer the lower bound $g_* \geq 2\sqrt{2}\, y_t(\Lambda_{\rm IR}) \approx 2.2$. The relation between the EW gauge couplings and the $SO(5)$ KK coupling is ($i = L, R$)

$$g_i(\Lambda_{\rm IR}) = g_*/\sqrt{kL(1 + r^2_{{\rm UV},i} + r^2_{{\rm IR},i})}\,, \tag{11}$$

where $r_{{\rm UV(IR)},i}$ is the contribution from boundary kinetic terms for the corresponding gauge bosons at the UV (IR) brane evaluated at the IR scale [40]. Taking for simplicity $r_{{\rm IR},i} = r_{{\rm UV},i} \equiv r_i$, $kL = 10$ and $g_* = 2.5$, we find that the EW gauge couplings are reproduced for $r_L \approx 0.5$ and $r_R \approx 1.4$.

II. *Other third-family Yukawas.* b and τ Yukawas, as well as the leading mixing among the light families and the third generation, are generated only after introducing IR-brane mass-mixing terms. The relevant IR masses are

$$\mathcal{L}_{\rm IR} \supset \bar{\Psi}^3_L \tilde{M}^L_{\Psi d} \mathcal{P}_L \Psi^3_{dR} + \bar{\mathcal{X}}_L (\tilde{M}^L_{\chi d} \mathcal{P}_L + \tilde{M}^R_{\chi d} \mathcal{P}_R) \Psi^3_{dR}$$
$$+ \bar{\Psi}^j_L \tilde{m}^R_{\Psi j} \mathcal{P}_R \Psi^3_R + \bar{\Psi}^j_L (\tilde{m}^L_{dj} \mathcal{P}_L + \tilde{m}^R_{dj} \mathcal{P}_R) \Psi^3_{dR}\,, \tag{12}$$

where we ignored the mass term between the $SU(2)_R$ components of Ψ^3 and χ, as well as those with $\Psi^{1,2}_{u,d}$, which have a minor phenomenological impact. These generate Yukawas between zero modes of the form

$$y_{f1f2} = \frac{g_*}{2\sqrt{2}}\, (\tilde{M}^L_{12} - \tilde{M}^R_{12})\, P\big(\{c^{(n)}_{f_1}\}, \{c^{(n)}_{f_2}\}\big)\,, \tag{13}$$

f_1 and f_2 denoting two generic 5D fermions, and $\tilde{M}^{L(R)}_{12}$ a generic IR mass between their $SU(2)_{L(R)}$ components. As anticipated, the hierarchies between these and the top Yukawa are fully explained by appropriate fermion localizations. For the benchmark in (6), we find

$$P\big(\{c^{(n)}_{\Psi^j}\}, \{c^{(n)}_{\Psi^3}\}\big) \sim e^{k(\ell_j - L)/2} \approx V_{j3}\,,$$
$$P\big(\{c^{(n)}_{\Psi^3,\mathcal{X}}\}, \{c^{(n)}_{\Psi^3_d}\}\big) \sim e^{k(\ell - L)/2} \approx y_b\,, \tag{14}$$
$$P\big(\{c^{(n)}_{\Psi^j}\}, \{c^{(n)}_{\Psi^3_d}\}\big) \sim e^{k(\ell + \ell_j - 2L)/2} \approx V_{j3}\, y_b\,,$$

where we used that $y_b \approx V_{23}$, with y_b the bottom Yukawa. Interestingly, we get a down-aligned limit (i.e. vanishing light-heavy entries in the down sector) in the $SO(5)$ symmetric limit, where $M^L_i = M^R_i$. Due to the chosen fermion BCs, an analogous limit in the up sector is not possible.

III. *Light-family Yukawas.* Due to the assumed strong UV localization of $\Psi^{1,2}_{u,d}$, light-family Yukawas are dominantly generated via their coupling with Σ. The relevant 5D proto-Yukawas are

$$\mathcal{L} \supset -Y^{ij}_{u,d}\, \bar{\Psi}^i\, \Sigma^a\, \Gamma^a\, P_R \Psi^j_{u,d}\,, \tag{15}$$

with Γ^a ($a = 1,\ldots,5$) being the $SO(5)$ gamma matrices. These proto-Yukawas can be in the bulk and (or) localized in the branes. The Σ field decomposes under the EW symmetry as a Higgs H' and a singlet S, and acquires a vacuum expectation value (VEV) along the singlet direction with an IR-localized profile. This breaking of $SO(5)$ generates light-family Yukawas suppressed by the Σ profile. Taking the Σ bulk mass close to the Breitenlohner-Freedman stability bound [41,42], we find

$$y^{ij}_{u,d} \approx \frac{g_*}{2\sqrt{2}}\, \tilde{Y}^{ij}_{u,d}\, \frac{\langle \Sigma_{\rm IR}\rangle}{\Lambda_{\rm IR}}\, e^{-k(L-\ell_j)}$$
$$\times\, e^{-k(c^{(1)}_i - \frac{1}{2})|y_i - \ell_j|}\, e^{k(c^{(1)}_j + \frac{1}{2})|y_j - \ell_j|}\,, \tag{16}$$

where $y_{i(j)}$ denotes the position of the brane where the left-handed (right-handed) field is dominantly localized, $c^{(1)}_{i(j)}$ is the left-handed (right-handed) 12-bulk mass in units of k, and $\tilde{Y}^{ij}_{u,d}$ are $\mathcal{O}(1)$ linear combinations of the proto-Yukawa couplings with coefficients depending on k, ℓ_i, the fermion bulk masses, and the Σ boundary masses (see (B.1)).

2.2. Higgs potential and EW precision data

The Higgs potential receives two types of contributions: i) a tree-level one resulting from the spontaneous breaking of the bulk gauge symmetry via Σ and Ω VEVs, and ii) a loop-level one from a finite volume effect due to non-local operators generated by 5D loops stretching from one boundary to the other [43]. In our model, the loop contribution comes dominantly from Ψ^3 and the EW gauge bosons. For small h/f, the Higgs potential is well approximated as

$$V(h) \approx \alpha(h)\cos\left(\frac{h}{f}\right) - \beta(h)\sin^2\left(\frac{h}{f}\right), \tag{17}$$

where $f \approx 2\Lambda_{\rm IR}/g_*$ is the Higgs decay constant, $\alpha(h) \approx \alpha_\Omega + \alpha_{\Psi^3}(h)$ and $\beta(h) \approx \beta_\Sigma + \beta_{\rm EW} + \beta_{\Psi^3}(h)$. Using a holographic approach cross-checked by the spectral function method, we find the following expressions for the coefficients α_i and β_i [44]

$$\begin{aligned}
\alpha_{\Psi^3}(h) &\approx \frac{3N_c f^4}{32\pi^2}\zeta(3)\, y_t^2 g_*^2 - 2\beta_{\Psi^3}(h)\,, \\
\alpha_\Omega &\approx (\tilde M_\Omega^R - \tilde M_\Omega^L)\,\Lambda_{\rm IR}^2 \langle\Omega_{\rm IR}\rangle^2\,, \\
\beta_{\Psi^3}(h) &\approx \frac{N_c f^4}{16\pi^2}\, y_t^4 \left[\gamma + \log\frac{\Lambda_{\rm IR}^2}{m_t^2(h)}\right], \\
\beta_{\rm EW} &\approx -\frac{9f^4}{512\pi^2}\, g_*^2\,\zeta(3)\left(3g_L^2 + g_Y^2\right), \\
\beta_\Sigma &\approx \frac{1}{2}(\tilde M_{H'} - \tilde M_S)\frac{\Lambda_{\rm IR}^2}{(kL)^2}\langle\Sigma_{\rm IR}\rangle^2\,,
\end{aligned} \tag{18}$$

where $\gamma \approx 0.38$, $\zeta(3) \approx 1.20$, $g_{L(Y)}$ is the $SU(2)_L$ ($U(1)_Y$) gauge coupling, $\langle\Omega_{\rm IR}\rangle$ and $\langle\Sigma_{\rm IR}\rangle$ are IR VEVs, $\tilde M_\Omega^{L(R)}$ are IR masses for the $SU(2)_{L(R)}$ components of Ω, and $\tilde M_{H',S}$ are UV masses for Σ (all masses in units of k). Approximating α and β as constants, the minimum of the potential and the Higgs mass are given by

$$\cos(\langle h\rangle/f) = -\frac{\alpha}{2\beta}\,, \qquad m_h^2 \equiv 2\lambda\langle h\rangle^2 \approx \frac{2\beta\langle h\rangle^2}{f^4}\,. \tag{19}$$

As we can see, the loop contributions $\alpha_{\Psi^3}, \beta_{\Psi^3}, \beta_{\rm EW}$ are completely fixed once a value for g_* (which also enters in the top Yukawa) is specified. Interestingly, we find that the coefficients α_i and β_i are of the right size such that the Higgs quartic comes out at the observed value for a natural choice of the undetermined tree-level parameters [45]. While the α_i and β_i are all of the same order, obtaining the required hierarchy between $\langle h\rangle$ and f implies a tuning of the parameters (the so-called little hierarchy problem), which is at the per mille level for $\Lambda_{\rm IR} = 8$ TeV and $g_* = 2.5$. We have verified that the results of this simplified computation hold up to small corrections when treating the full loop potential numerically including all fields dominantly localized in the IR, as well as the relevant IR boundary masses.

Additionally, our theory predicts a tower of KK vector resonances which couple dominantly to the IR localized fields. The most dangerous of these states are those that mix with the SM EW gauge bosons, as they induce g_*/g_L enhanced modifications to their couplings with third generation SM fermions. Resumming the KK tower, we find corrections of the form

$$\frac{\delta g_{Z\Psi^3\Psi^3}}{g_{Z\Psi^3\Psi^3}} \approx -0.3\frac{m_Z^2}{M_{\rm KK}^2}\frac{g_*^2}{g_L^2} \approx -\frac{0.3}{4c_W^2}\frac{\langle h\rangle^2}{f^2}\,, \tag{20}$$

where c_W is the cosine of the Weinberg angle and the pre-factor of 0.3 comes dominantly from the Higgs and Ψ^3 profiles. The strongest bound comes from $Z \to \tau_L\tau_L$, leading to a constraint on (20) at the per-mille level [46], which is well satisfied for our benchmark point.

3. Conclusions

We have presented a UV extension of the SM that addresses two of its long-standing open issues: the origin of flavor hierarchies and the stabilization of the Higgs sector, while, at the same time, explaining the observed anomalies in B decays. A coherent solution to these three problems is obtained by embedding the SM into a warped 5D construction with three (flat) four-dimensional branes, where each SM family is quasi-localized. The 3-brane structure, which lets us associate flavor indices to well-defined positions in the extra dimension, is a crucial distinction from previous explanations of the flavor hierarchies in the context of warped extra dimensions [40,47–49]. This structure results in an approximate $U(2)^n$ flavor symmetry with leading breaking in the left-handed sector, which is necessary in order to evade the tight bounds on new physics from flavor-changing processes while simultaneously addressing the B anomalies [13,19].

We emphasize that the explicit model analyzed here is part of a larger class of theories, based on the three fundamental points presented in the Introduction. A few building blocks, such as the choice of the IR-bulk and UV-brane symmetries, are motivated by observations. Other aspects (especially those related to UV dynamics) are less constrained and could be modified. The geometry itself is a minimal choice, and the validity of the construction could be extended up to the Planck scale by adding an additional UV brane, solving the large EW hierarchy problem as in the original RS model [37].

By construction, the TeV-scale phenomenology of this model is equivalent to that of 4321 models discussed in the recent literature [22–24]. However, deviations are expected around $M_{\rm KK} \sim 10$ TeV due to the tower of KK states. A further striking signature, specific of the multi-scale (multi-brane) structure of the theory, is a multi-peaked stochastic gravitational wave signal potentially within reach of future experiments, originating from a series of phase transitions in the early universe [50].

Declaration of competing interest

The authors declare that they have no known competing financial interests or personal relationships that could have appeared to influence the work reported in this paper.

Data availability

No data was used for the research described in the article.

Acknowledgements

This project has received funding from the European Research Council (ERC) under the European Union's Horizon 2020 research and innovation programme under grant agreement 833280 (FLAY), and by the Swiss National Science Foundation (SNF) under contract 200020_204428. The work of JF has been supported by the Spanish Ministry of Science and Innovation (MCIN) and the European Union NextGenerationEU/PRTR under grant IJC2020-043549-I, by the MCIN grant PID2019-106087GB-C22, and by the Junta de Andalucía grants P18-FR-4314 (FEDER) and FQM101.

Appendix A. General profile function

The profile function introduced in the main text is given by

$$P\left(\{c_L^{(n)}\},\{c_R^{(n)}\}\right) \equiv p\left(\{c_L^{(n)}\}\right)p\left(\{-c_R^{(n)}\}\right), \tag{A.1}$$

where, in the two bulk case with $k_1 = k_2 \equiv k$, we have

$$p(\{c_1, c_2\}) = \sqrt{\frac{(1-2c_1)(1-2c_2)}{(1-2c_1) - e^{2k(L-\ell)(c_2-1/2)}\left[(1-2c_2)\,e^{2k\ell(c_1-1/2)} + 2(c_2-c_1)\right]}}\,, \tag{A.2}$$

with ℓ being the location of the intermediate brane. Some interesting cases are: $p\big(\{0,0\}\big) \approx 1$, $p\big(\{1/2,1/2\}\big) \approx \frac{1}{\sqrt{kL}}$, and $p\big(\{0,1\}\big) \approx \frac{1}{\sqrt{2}}\,e^{-k(L-\ell)/2}$, $p\big(\{1,1\}\big) \approx e^{-kL/2}$.

Appendix B. Light-Yukawa couplings

The parameters appearing in the light-Yukawa couplings formula (16) are

$$\begin{aligned}
\tilde{Y}^{i2}_{u,d} =& 2\sqrt{2}\frac{\ell}{L}\,N_{y_i}(\{c_i^{(n)}\})N_{y_{c,s}}(\{-c_{c,s}^{(n)}\})\left(\frac{\sqrt{k}\,Y^{i2\,(1)}_{u,d}}{2-c_i^{(1)}+c_{c,s}^{(1)}}\right.\\
&\left.+\frac{\sqrt{k}\,Y^{i2\,(2)}_{u,d}}{-2+c_i^{(2)}-c_{c,s}^{(2)}}+\sqrt{k^3}\,Y''^{i2}_{u,d}\right)+\mathcal{O}\left(\frac{1}{kL}\right),\\
\tilde{Y}^{i1}_{u,d} =& \frac{2\sqrt{2}}{kL}\,N_{y_i}(\{c_i^{(n)}\})N_{y_{u,d}}(\{-c_{u,d}^{(n)}\})\frac{1}{2\left(\tilde{M}_{H'}+2\right)}\\
&\times\left[\sqrt{k}\,Y^{i1(1)}_{u,d}\frac{6-c_i^{(1)}+c_{u,d}^{(1)}+2\tilde{M}_{H'}}{\left(2-c_i^{(1)}+c_{u,d}^{(1)}\right)^2}-\sqrt{k^3}\,Y'^{i1}_{u,d}\right]\\
&+\mathcal{O}\left(\frac{1}{k^2L^2}\right),
\end{aligned} \tag{B.1}$$

where $Y^{ij(1,2)}_{u,d}$ are the 12- and 23-bulk proto-Yukawas, $Y'^{ij}_{u,d}$ ($Y''^{ij}_{u,d}$) are the first (second) brane proto-Yukawas, $c_i^{(1,2)}$ ($c_{u,d,c,s}^{(1,2)}$) are the left-handed (right-handed) fermion 5D masses in the 12- and 23-bulk in units of k, y_i ($y_{u,d,c,s}$) is the position of the brane where the left-handed (right-handed) fermions is mainly localized, and

$$N_y(\{c^{(n)}\}) = \begin{cases} \sqrt{-1+2c^{(1)}} & \text{if } y = 0 \\ \sqrt{\frac{(-1+2c^{(1)})(-1+2c^{(2)})}{2\,(c^{(1)}-c^{(2)})}} & \text{if } y = \ell \end{cases}. \tag{B.2}$$

References

[1] LHCb Collaboration, R. Aaij, et al., Test of lepton universality using $B^+ \to K^+\ell^+\ell^-$ decays, Phys. Rev. Lett. 113 (2014) 151601, arXiv:1406.6482.

[2] LHCb Collaboration, R. Aaij, et al., Test of lepton universality with $B^0 \to K^{*0}\ell^+\ell^-$ decays, J. High Energy Phys. 08 (2017) 055, arXiv:1705.05802.

[3] LHCb Collaboration, R. Aaij, et al., Search for lepton-universality violation in $B^+ \to K^+\ell^+\ell^-$ decays, Phys. Rev. Lett. 122 (19) (2019) 191801, arXiv:1903.09252.

[4] LHCb Collaboration, R. Aaij, et al., Test of lepton universality in beauty-quark decays, arXiv:2103.11769.

[5] BaBar Collaboration, J.P. Lees, et al., Evidence for an excess of $\bar{B} \to D^{(*)}\tau^-\bar{\nu}_\tau$ decays, Phys. Rev. Lett. 109 (2012) 101802, arXiv:1205.5442.

[6] BaBar Collaboration, J.P. Lees, et al., Measurement of an excess of $\bar{B} \to D^{(*)}\tau^-\bar{\nu}_\tau$ decays and implications for charged Higgs bosons, Phys. Rev. D 88 (7) (2013) 072012, arXiv:1303.0571.

[7] Belle Collaboration, M. Huschle, et al., Measurement of the branching ratio of $\bar{B} \to D^{(*)}\tau^-\bar{\nu}_\tau$ relative to $\bar{B} \to D^{(*)}\ell^-\bar{\nu}_\ell$ decays with hadronic tagging at Belle, Phys. Rev. D 92 (7) (2015) 072014, arXiv:1507.03233.

[8] LHCb Collaboration, R. Aaij, et al., Measurement of the ratio of branching fractions $\mathcal{B}(\bar{B}^0 \to D^{*+}\tau^-\bar{\nu}_\tau)/\mathcal{B}(\bar{B}^0 \to D^{*+}\mu^-\bar{\nu}_\mu)$, Phys. Rev. Lett. 115 (11) (2015) 111803, arXiv:1506.08614, Erratum: Phys. Rev. Lett. 115 (2015) 159901.

[9] LHCb Collaboration, R. Aaij, et al., Measurement of the ratio of the $B^0 \to D^{*-}\tau^+\nu_\tau$ and $B^0 \to D^{*-}\mu^+\nu_\mu$ branching fractions using three-prong τ-lepton decays, Phys. Rev. Lett. 120 (17) (2018) 171802, arXiv:1708.08856.

[10] LHCb Collaboration, R. Aaij, et al., Test of lepton flavor universality by the measurement of the $B^0 \to D^{*-}\tau^+\nu_\tau$ branching fraction using three-prong τ decays, Phys. Rev. D 97 (7) (2018) 072013, arXiv:1711.02505.

[11] M. Bordone, C. Cornella, J. Fuentes-Martin, G. Isidori, A three-site gauge model for flavor hierarchies and flavor anomalies, Phys. Lett. B 779 (2018) 317–323, arXiv:1712.01368.

[12] A. Greljo, G. Isidori, D. Marzocca, On the breaking of lepton flavor universality in B decays, J. High Energy Phys. 07 (2015) 142, arXiv:1506.01705.

[13] R. Barbieri, G. Isidori, A. Pattori, F. Senia, Anomalies in B-decays and $U(2)$ flavour symmetry, Eur. Phys. J. C 76 (2) (2016) 67, arXiv:1512.01560.

[14] R. Barbieri, A. Tesi, B-decay anomalies in Pati-Salam SU(4), Eur. Phys. J. C 78 (3) (2018) 193, arXiv:1712.06844.

[15] J. Fuentes-Martín, P. Stangl, Third-family quark-lepton unification with a fundamental composite Higgs, Phys. Lett. B 811 (2020) 135953, arXiv:2004.11376.

[16] R. Alonso, B. Grinstein, J. Martin Camalich, Lepton universality violation and lepton flavor conservation in B-meson decays, J. High Energy Phys. 10 (2015) 184, arXiv:1505.05164.

[17] L. Calibbi, A. Crivellin, T. Ota, Effective field theory approach to $b \to s\ell\ell^{(')}$, $B \to K^{(*)}\nu\overline{\nu}$ and $B \to D^{(*)}\tau\nu$ with third generation couplings, Phys. Rev. Lett. 115 (2015) 181801, arXiv:1506.02661.

[18] B. Bhattacharya, A. Datta, J.-P. Guévin, D. London, R. Watanabe, Simultaneous explanation of the R_K and $R_{D^{(*)}}$ puzzles: a model analysis, J. High Energy Phys. 01 (2017) 015, arXiv:1609.09078.

[19] D. Buttazzo, A. Greljo, G. Isidori, D. Marzocca, B-physics anomalies: a guide to combined explanations, J. High Energy Phys. 11 (2017) 044, arXiv:1706.07808.

[20] L. Di Luzio, A. Greljo, M. Nardecchia, Gauge leptoquark as the origin of B-physics anomalies, Phys. Rev. D 96 (11) (2017) 115011, arXiv:1708.08450.

[21] A. Greljo, B.A. Stefanek, Third family quark–lepton unification at the TeV scale, Phys. Lett. B 782 (2018) 131–138, arXiv:1802.04274.

[22] L. Di Luzio, J. Fuentes-Martin, A. Greljo, M. Nardecchia, S. Renner, Maximal flavour violation: a Cabibbo mechanism for leptoquarks, J. High Energy Phys. 11 (2018) 081, arXiv:1808.00942.

[23] C. Cornella, J. Fuentes-Martin, G. Isidori, Revisiting the vector leptoquark explanation of the B-physics anomalies, J. High Energy Phys. 07 (2019) 168, arXiv:1903.11517.

[24] C. Cornella, D.A. Faroughy, J. Fuentes-Martin, G. Isidori, M. Neubert, Reading the footprints of the B-meson flavor anomalies, J. High Energy Phys. 08 (2021) 050, arXiv:2103.16558.

[25] G. Panico, A. Pomarol, Flavor hierarchies from dynamical scales, J. High Energy Phys. 07 (2016) 097, arXiv:1603.06609.

[26] L. Allwicher, G. Isidori, A.E. Thomsen, Stability of the Higgs sector in a flavor-inspired multi-scale model, J. High Energy Phys. 01 (2021) 191, arXiv:2011.01946.

[27] R. Barbieri, A view of flavour physics in 2021, Acta Phys. Pol. B 52 (6–7) (2021) 789, arXiv:2103.15635.

[28] J. Fuentes-Martin, G. Isidori, J. Pagès, B.A. Stefanek, Flavor non-universal Pati-Salam unification and neutrino masses, Phys. Lett. B 820 (2021) 136484, arXiv:2012.10492.

[29] R. Contino, Y. Nomura, A. Pomarol, Higgs as a holographic pseudoGoldstone boson, Nucl. Phys. B 671 (2003) 148–174, arXiv:hep-ph/0306259.

[30] K. Agashe, R. Contino, A. Pomarol, The minimal composite Higgs model, Nucl. Phys. B 719 (2005) 165–187, arXiv:hep-ph/0412089.

[31] I.I. Kogan, S. Mouslopoulos, A. Papazoglou, G.G. Ross, Multi-brane worlds and modification of gravity at large scales, Nucl. Phys. B 595 (2001) 225–249, arXiv:hep-th/0006030.

[32] W.D. Goldberger, M.B. Wise, Modulus stabilization with bulk fields, Phys. Rev. Lett. 83 (1999) 4922–4925, arXiv:hep-ph/9907447.

[33] S.J. Lee, Y. Nakai, M. Suzuki, Multiple hierarchies from a warped extra dimension, J. High Energy Phys. 02 (2022) 050, arXiv:2109.10938.

[34] In the limit of $k_1\ell, k_2(L-\ell) > 1$ and small bulk mass for the GW scalar, the stabilization is achieved via two factorized solutions of the type found in [32], one for each distance.

[35] Assuming no boundary kinetic terms for $SU(4)_h \times SU(3)_\ell \times U(1)_{\ell+R}$ part of the gauge symmetry.

[36] These global $U(1)$ symmetries could instead be gauge bulk symmetries broken at a deeper UV brane (like the Planck brane). In this case, anomaly cancellation requires UV-brane fermions with masses at the symmetry breaking scale.

[37] L. Randall, R. Sundrum, A large mass hierarchy from a small extra dimension, Phys. Rev. Lett. 83 (1999) 3370–3373, arXiv:hep-ph/9905221.

[38] S.J. Huber, Q. Shafi, Fermion masses, mixings and proton decay in a Randall-Sundrum model, Phys. Lett. B 498 (2001) 256–262, arXiv:hep-ph/0010195.

[39] See supplementary material.

[40] C. Csaki, A. Falkowski, A. Weiler, The flavor of the composite pseudo-Goldstone Higgs, J. High Energy Phys. 09 (2008) 008, arXiv:0804.1954.

[41] P. Breitenlohner, D.Z. Freedman, Stability in gauged extended supergravity, Ann. Phys. 144 (1982) 249.

[42] P. Breitenlohner, D.Z. Freedman, Positive energy in anti-de Sitter backgrounds and gauged extended supergravity, Phys. Lett. B 115 (1982) 197–201.

[43] Y. Hosotani, Dynamical gauge symmetry breaking as the Casimir effect, Phys. Lett. B 129 (3) (1983) 193–197.

[44] In the tree-level computation, we assume large kL and neglect higher order terms in the boundary masses. For the loop via the spectral function, we include only Ψ^3 and EW gauge bosons, and we use approximate form factors as discussed in [51], which allow for an analytic computation.
[45] We expect $\langle \Sigma_{\rm IR} \rangle \approx \mathcal{O}(\Lambda_{\rm IR})$. However, due to the localization of Ω in the UV, we can naturally have $\langle \Omega_{\rm IR} \rangle \lesssim \Lambda_{\rm IR}$.
[46] A. Efrati, A. Falkowski, Y. Soreq, Electroweak constraints on flavorful effective theories, J. High Energy Phys. 07 (2015) 018, arXiv:1503.07872.
[47] Y. Grossman, M. Neubert, Neutrino masses and mixings in nonfactorizable geometry, Phys. Lett. B 474 (2000) 361–371, arXiv:hep-ph/9912408.
[48] A.E. Nelson, M.J. Strassler, Suppressing flavor anarchy, J. High Energy Phys. 09 (2000) 030, arXiv:hep-ph/0006251.
[49] K. Agashe, G. Perez, A. Soni, Flavor structure of warped extra dimension models, Phys. Rev. D 71 (2005) 016002, arXiv:hep-ph/0408134.
[50] A. Greljo, T. Opferkuch, B.A. Stefanek, Gravitational imprints of flavor hierarchies, Phys. Rev. Lett. 124 (17) (2020) 171802, arXiv:1910.02014.
[51] A. Falkowski, About the holographic pseudo-Goldstone boson, Phys. Rev. D 75 (2007) 025017, arXiv:hep-ph/0610336.